Indonesian Journal of Electrical Engineering and Computer Science
Vol. 3, No. 1, July 2016, pp. 215 ~ 225
DOI: 10.11591/ijeecs.v3.i1.pp215-225

Study on Characteristics of SAR Data in Ravine Reservoir Area

XIE Mowen[1*], Huang Jiaxuan[1], Huang Jiehui[2]
[1]School of Civil and Environmental Engineering, University of Science and Technology Beijing, Beijing 100083, China
[2]College of Civil Engineering and Architecture, Shandong University of Technology, Zibo, Shandong 255049, China
*Corresponding author, e-mail: mowenxie@ustb.edu.cn, lanting1224@gmail.com, jiehuizhifei@126.com

Abstract

Landslide monitoring is one of the most important methods in landslide prevention. Landslide early identifying that based on D-InSAR technique is one of the effective means in landslide monitoring in ravine reservoir area. On the basis of D-InSAR technique analysis in ravine reservoir, how to eliminate the error and find the real moving area caused by rock and soil is the key problem. Considering the fact, an experiment region in reservoir of Wudongde hydropower station, Jinsha River has been studied. Based on D-InSAR analysis method and the characteristics of radar data, an analysis method of the SAR data trusted zone, the detectable landsliding displacement and error estimation has been established, extracting the effective range in the result of SAR data analysis.

Keywords*: reservoir landslide, D-InSAR, characteristics of data, error estimation*

1. Introduction

Landslide formation and development is a very long process, which is difficult to identify by the naked eyes. Through capture the process of physical monitoring landslide disaster to find the landslide as soon as possible, provide the effectively early warning and prevention. The traditional warning methods rely on geological surveying, field exploration and long-term observation in a single landslide by human ability, which require a lot of manpower and resources. The on-site monitoring instruments include tiltmeter, displacement meter, stressmeter, water level gauge and GPS, TDR and other electronic remote monitoring technology [1-3]. These methods can provide important information about the location and displacement. The advantage is high accuracy of single point and the disadvantage is hard to set markers in the test area, it is hard to apply in the danger zone that people different to arrived. The process of traditional measurement method has the single point error of non-uniformity, it is not conductive to the overall trend of displacement analysis. Differential Synthetic Aperture Radar Interferometry (D-InSAR) technology plays a seminal role in the landslide early detection and monitoring.

D-InSAR technology is a new Earth-observation technique that detects surface movement at the subcentimeter level. The deformation results make up the shortcoming of traditional measurement methods of sparse points. D-InSAR technology can get the deformation of surface in tens of square kilometers. The advantages of D-InSAR technology contains: all-weather adaptability, coverage of inaccessible areas, low cost, and without monitoring network [4]. Thus, D-InSAR technology has been widely used in the landslide monitoring areas.

Gabriel et al. (1989) [5] measured surface deformation in the southeastern California Imperial Valley Irrigation District. They were the first to demonstrate that D-InSAR can be used to monitor surface deformation at the centimeter level. Early studies have focused on monitoring large movements caused by earthquakes or volcanoes. With the development of theoretical research, however, the focus has shifted to small ground movements such as ground subsidence and landslides. Achache et al. (1995) [6] demonstrated the capability of D-InSAR to monitor small displacements with the same accuracy as that of ground measurement. Berardino

Received February 2, 2016; Revised May 25, 2016; Accepted June 10, 2016

et al. (2003) [7] proposed a kinematic model of instability within the investigated time interval for the Maratea Valley landslide and acquired consistent data using a Global Positioning System (GPS) device. Colesanti et al. (2003) [8] combined the D-InSAR and permanent or persistent scatterers (PS) techniques to monitor Southern California and Ancona, and obtained 1 mm accuracy. These researchers also monitored areas covered with plants. Singhroy and Molch (2004) [9] analyzed debris flow characteristics, rock fall distribution, as well as landslide process and mobility through the D-InSAR and RADARSAT model. Catan, et al., (2005) [10] demonstrated that D-InSAR can quantitatively determine the nature of a terrain. Singhroy et al. (2006) [11] identified slope activities and their causes by analyzing different geological materials from the displacement of past landslides; they also adopted corner reflector (CR) techniques. Li, et al., (2000) [12] focused on the D-InSAR method, theory and its potential in analyzing surface deformation, including the slope. The China Geological Environment Monitoring Institute collaborated with the German Earth Environment Research Center in 2005 to monitor landslides using CRs and D-InSAR, which achieved a certain effect. However, the actual applications of landslide monitoring in China remain few.

Given the strict limitations of terrain, surface state and atmospheric effects, D-InSAR technology is unsuitable for ravine reservoir areas [13-14]. D-InSAR technology has some limitations and unsolved problems. The monitoring results by D-InSAR technology displayed a planar distribution that obtained different degrees of deformation in the whole study area. It is hard to identify the effective displacement caused by rock and soil. Current research demonstrated that D-InSAR technology can be used to detect the known landslides, but the causes of small deformation in the whole and how to eliminate the error caused by non-rock deformation still not been studied. In ravine reservoir area, SAR image susceptible to noise, surface topography, atmospheric status and other natural factors, which lead to the mass error of monitoring results and reduce the accuracy of data [15]. How to extract the effective SAR data and identify the credible zone in the study is also a problem to be solved.

This study combined SAR programming data with the topography of ravine area and through different shooting modes to eliminate limitation of the natural conditions, to extract the effective SAR data to ensure the credible zone in the study area. The study through error analysis of D-InSAR interferometry results to obtain the error value that caused by non-rock deformation (natural conditions, satellite orbit and other factors). By filter the error value in this range to obtain real landslide movement deformation and achieve the purpose of landslide monitoring.

The study area is Jinsha River Wudongde Hydropower Reservoir. This paper based on geological survey and result of preliminary remote sensing research, through the analysis of different topographic factors on D-InSAR data to obtain the credible zone in study area. River as PS points and CR points have been taken to estimation the error value range of monitoring data. This method provided the theoretical foundation for landslide early detection and provided technical support for large hydropower project on geological disaster monitoring and public safety monitoring.

2. Study Area And Data Selection

2.1. Study Area

The center coordinate of the study area is 102°36′N, 26°22′E, which is located near the dam site of the Wudongde Hydropower Reservoir. This hydropower reservoir is found at the junction of Luquan County in Yunnan Province and Huidong Country in Sichuan Province, China. It is one of the key projects of west-east gas pipeline project. Wudongde Hydropower Reservoir is a typical area in the southwest ravine reservoir area. The study area and the main landslide distribution show in Figure 1.

2.2. SAR Data Selection

Rainfall is one of the main factors of landslide disaster, landslide moving fast in the rainy season. In order to monitoring the deformation before and after rainy season, the authors set the shooting time from May to September.

Given the characteristics of radar remote sensing lateral imaging, SAR images have foreshortening, top and bottom displacement (TBD) and shadows [16-17]. The angle of the surrounding mountains was observed to determine the incident (IA), which excluded the effects

of TBD and shadows. TBD is an extreme foreshortening phenomenon that only occurs when the slope is facing toward the shooting direction and the IA is less than the local terrain. The generation condition of shadows is the radar beam angle of depression, which is less than the back slope gradient angle that only occurs in the back slope. Avoiding shadows in a large topography area to improve the data reliability is necessary.

The Jinpingzi landslide and its surroundings are the major monitoring area. Three cross-sectional views are shown in Figure 2. The IA should be larger than the slope gradient angle (SGA). Moreover, the sum of the radar beam angle and the back slope gradient angle (BSGA) should be less than 90° to avoid top and bottom displacement and shadows. Figure 2 shows the front slope gradient angle (FSGA) value and the BSGA value of three cross sectional, the IA should be larger than the FSGA (α) and less than the BSGA (β). Thus, the satellite IA is 40°.

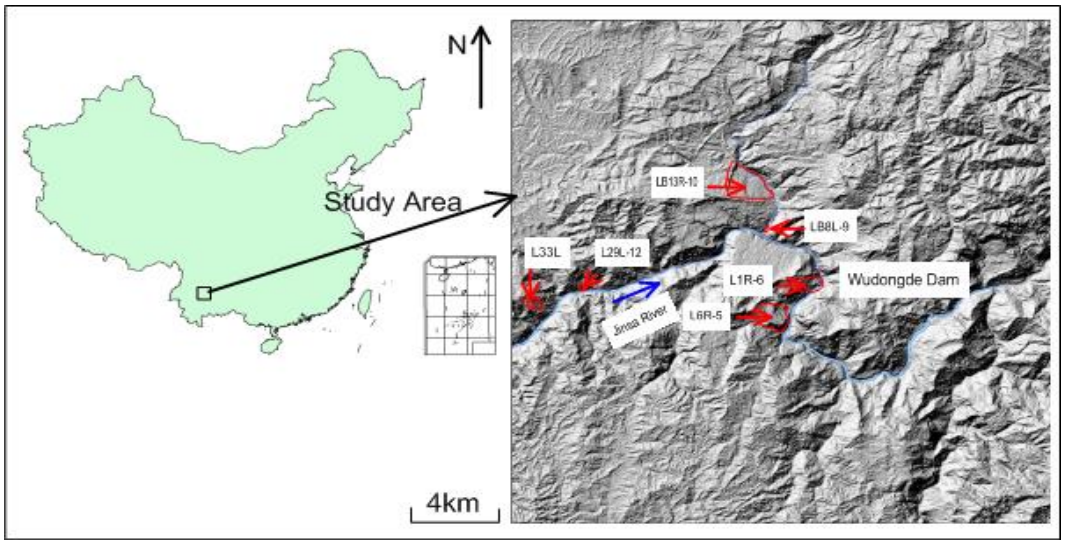

Figure 1. Study Area and Landslide Distribution Map

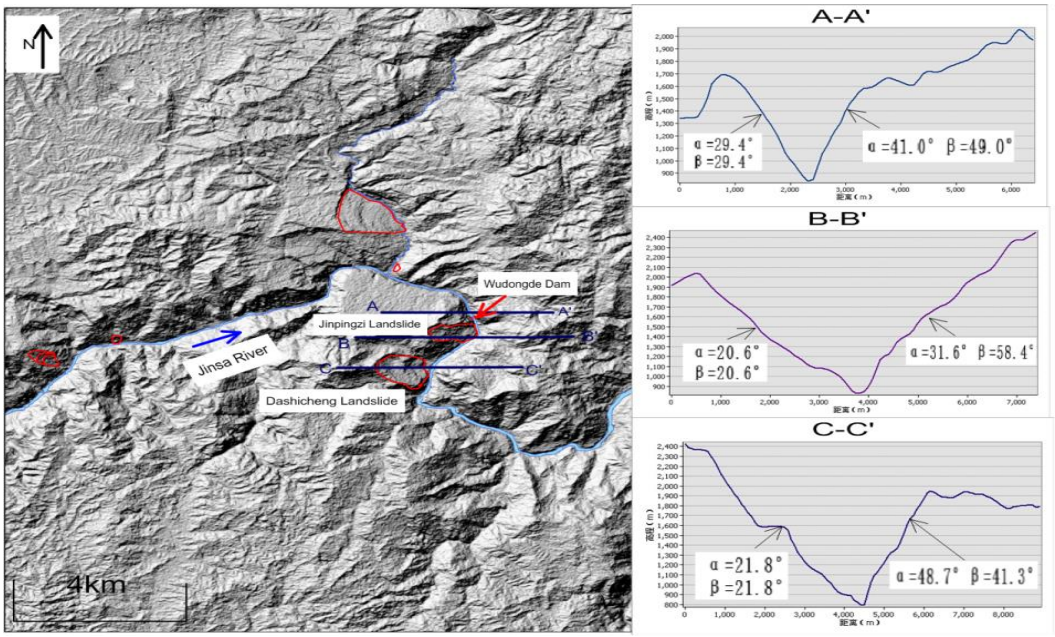

Figure 2. Section That Focuses on the Study Area

The descending orbit direction of the RADARSAT-2 satellite is from northeast to southwest, whereas the ascending orbit direction is from southeast to northwest. The shooting mode shows in Figure 3. All directions are in the right view. The study area slope is directed toward the east; thus, the descending orbit is the best option. The descending and ascending orbit program data in 2011 were adopted to demonstrate the results of different times and cover all study areas effectively.

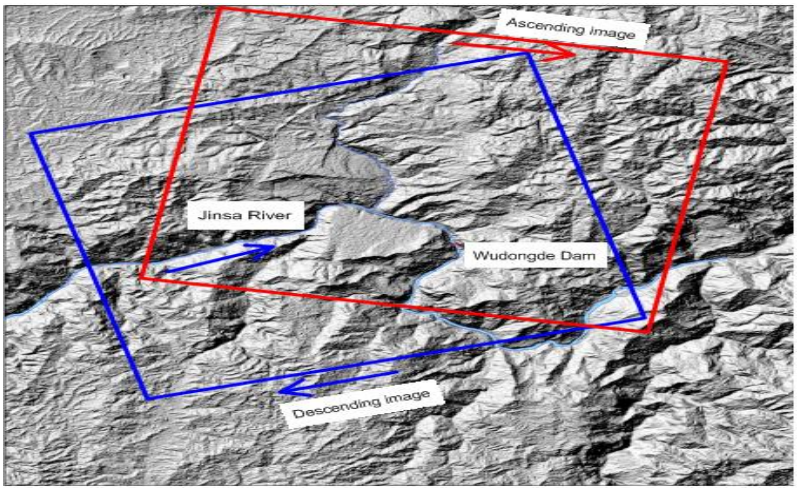

Figure 3. Ascending Range and Descending Range

Considering all the aforementioned factors, we ordered 8 images from the descending orbit data in 2010 (from May to November), 5 images from the descending orbit data in 2011 (from March to April and from July to September), and 3 images from the ascending orbit data in 2011 with horizontal–horizontal (HH) polarization, 3 m resolution, a shooting scope of 20 km × 20 km, and the IA is 39.57°.

3. D-InSAR Data Analysis

One of the interferential images that contain ground deformation is shown in Figure 4. The deformation occurred from May 15th, 2010 to July 4th, 2010. The negative value indicates the leaving satellite direction. Different degrees of surface deformation in the entire area are shown in the map, but whether displacement was caused by landslides and how interferential error can be filter to identify moving landslides still not be determined. After years of research on SAR data analysis, the authors found the methods to elimination the systematic error that caused by topographical features, satellite orbit and other natural factors.

3.1. Effect of Local Incident Angle on SAR Data

SAR remote sensing and its interferential results are closely related to the topography and surface reflection characteristics of the ravine reservoir area. Thus, understanding SAR remote sensing and its differential interferometry features is necessary to determine the effective range of SAR data analysis. Based on analyze the relationship between SAR data backward scattering (BS), coherence coefficient (CC), ascending and descending orbit and topography features to find the credible zone.

The local incident angle (LIA) is a key factor in this research because the close relationship between BS and the SAR technique relies on the principle of BS [18]. Identifying the relationship between the local incident angle and BS, as well as between LIA and CC, is necessary.

LIA is the angle between the sightline of satellite (Vs) and the surface normal (Vn). As shown in Figure 5, α is the slope gradient angle, θ is the satellite IA, θloc is LIA.

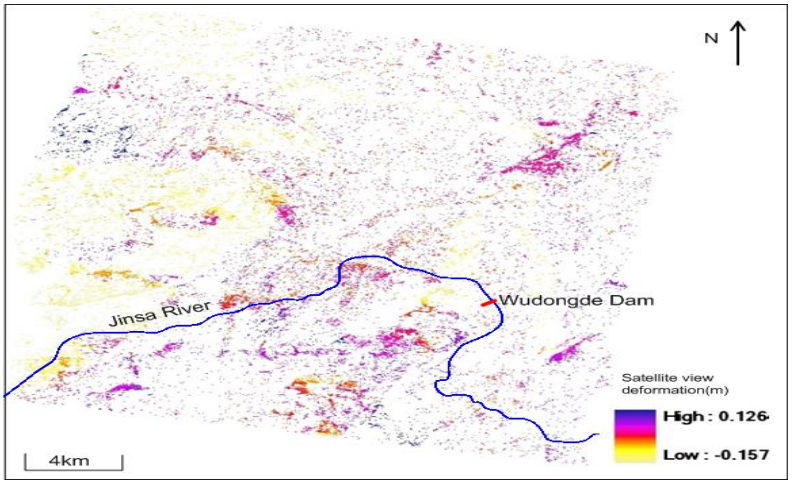

Figure 4. Surface Deformation Map (m)

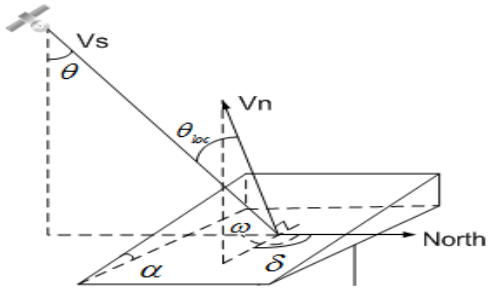

Figure 5. Schematic of Local Incidence Angle

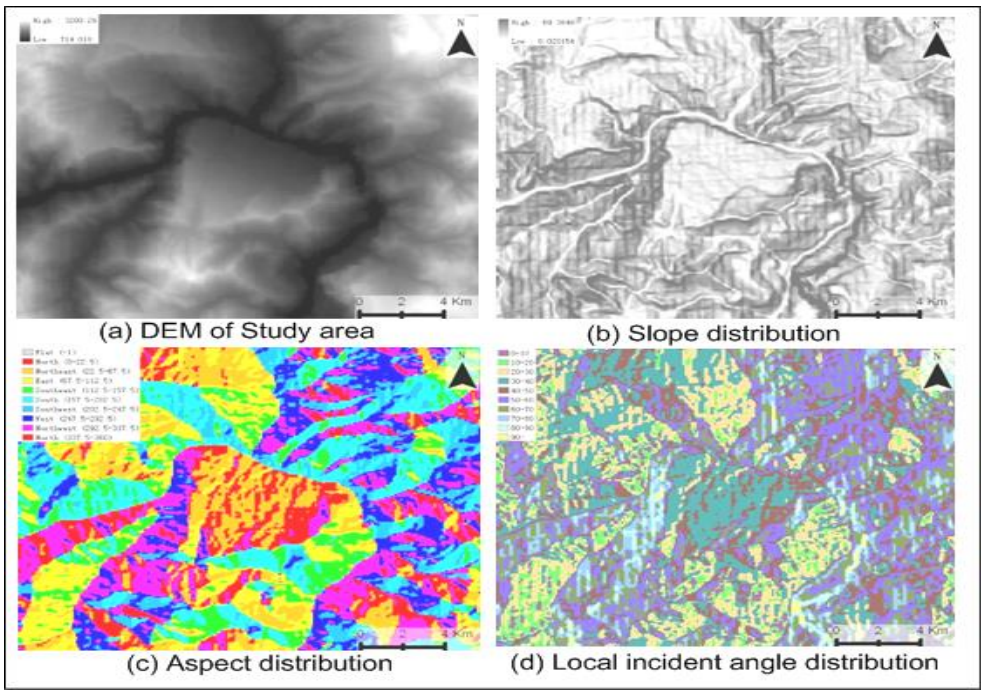

Figure 6. Schematic of Study Area Local Incidence Angle

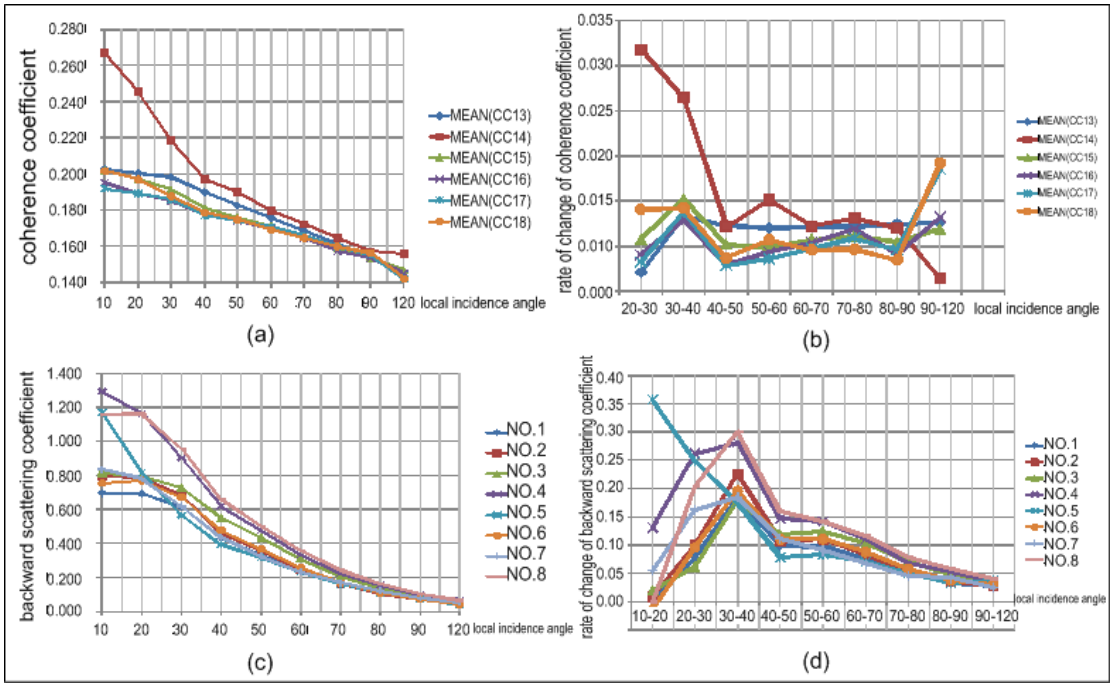

Figure 7 (a) Local Incident Angle and Coherence Coefficient Graph, (b) Local Incident Angle and Rate of Change in the Coherence Coefficient Graph, (c) Local Incident Angle and Backward Scattering Coefficient Graph, (d) Local Incidence Angle and Rate of Change in the Backward Scattering Coefficient Graph

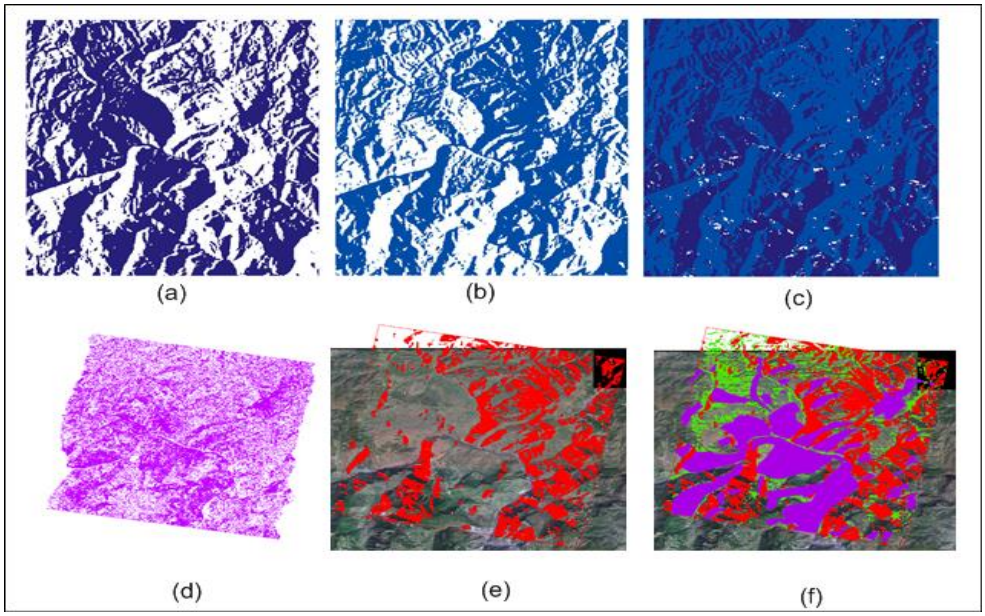

Figure 8. Credible Zone Distribution of SAR Data, (a)(b)(c) According to the Local Incidence Angle Calculated Ascending (left), Descending (middle) and Overlapping (right), Amounting to more than 98%, (d)(e)(f) According to the Coherence Calculated Ascending (left), Descending (middle) and Overlapping (right), Amounting to more than 91%

The IA of RADARSAT-2 descending orbit data is 39.83°, whereas its azimuth is 189.48°. Through the spatial analysis of DEM in study area (Figure 6(a)) obtained slope distribution (Figure 6(b)) and aspect distribution (Figure 6(c)). LIA is determined by sight

parameters of satellite, slope and aspect (Figure 6(d)). LIA classified per 10 degrees as a group, as shown in Figure 7 means the relationship between LIA and the average of CC and BS. The LIA and the CC graph are shown in Figure 7(a). The LIA and rate of change in the CC graph are shown in Figure 7(b). The LIA and the BS graph are shown in Figure 7(c). The LIA and the rate of change in the BS graph are shown in Figure 7(d). These graphs indicate the close relationship between the CC, BS and the LIA. The CC and BS decreased with the increasing LIA. These trends indicate that the LIA is approximately 40° to 50°. The LIA of 50° is considered as the credible zone.

3.2. SAR Data Credible Zone

Various satellite shooting modes results in different areas with layovers and shadows [19]. Thus, the monitoring results of these areas are unreliable. The overlapping (mix of ascending and descending operations) calculation method is an effective approach to monitor a study area. As shown in Figure 8(a), 8(b), and 8(c), the overlapping calculation method and the credible zone covered over 98% based on the LIA of 50°. As shown in Figure 8(d), 8(e), and 8(f), the overlapping calculation method and the credible zone covered over 91% based on the calculated CC of 0.18. The proposed method is effective by using overlapping calculation. The results shown in Figure 8 combined ascending and descending orbit shooting modes, and the credible zone covered the entire study area.

4. Error Analysis

The D-InSAR technique uses phase measurements to obtain the characteristics of the target area and deformation information. An interferometric image contains topographic information, surface information, and phase delay caused by atmospheric activities that are sensitive to micro-deformation [20]. If the deformation is not caused by landslide movement, it will directly influence the differential results.

4.1. Error Sources Analysis of D-InSAR Monitoring Results

D-InSAR technology is widely used in landslide monitoring, but due to restriction of many factors it has not mature yet, there is a big error. It is necessary to analysis where are the errors come from.

4.1.1. Atmospheric Effect

Due to the factors such as clouds, atmospheric and ionosphere caused radar echo signal phase delay phenomenon called atmospheric delay [21]. In the three-pass method, the three imaging time interval for several cycles. In the imaging observation time, the influence of atmospheric fluctuations, especially tropospheric humidity and temperature changes, produced the different phase delay. D-InSAR monitoring tiny deformation, the phase delay shows in the deformation map as error value, which reduces the accuracy of D-InSAR monitoring results.

Using two-frequency or multi-frequency observation methods can reduce the influence of ionosphere on D-InSAR monitoring results, but water vapor changes dramatically in tropospheric and irregularity. Thus, the influence of tropospheric activity for SAR monitoring accuracy became one of difficult problems on D-InSAR monitoring technical.

4.1.2. Phase Decorrelation

Phase decorrelation is a serious problem that limits the application of the D-InSAR technique [22]. Besides baseline length and slightly non-parallel tracks, other external conditions can also lead to phase decorrelation, such as time, rapid movement, cover plant, air-conditioners, humidity and excessive landslide deformation. Selecting reasonable data increases their relevance. Phase decorrelation divided into spatial decorrelation, time decorrelation and target decorrelation.

During the heavy rail shooting model, satellite shot many times on the same area. The two any two shots spatial positions were unable to achieve coincidence. The space position changes caused geometry changes, echo phase shift. This phenomenon called spatial decorrelation. Time decorrelation is mainly due to the changes of target coherent scattering characteristics, access to signal decorrelation in the same area.

In summary, although D-InSAR monitoring method with high precision in theoretical, but under the influence of various conditions, the error is large. There are several methods to solve the problems about atmospheric delay and phase decorrelation: First, unwrapping under conditions of low coherence. Second, deformation phase and atmospheric delay phase separation in deformation phase. The former is used a small amount of interferometric phase to restore the real phase, needs discrete phase unwrapping to inverse the surface changes. The latter is separated atmospheric delay phase from interferometric phase to improve the accuracy of calculated volume. Although D-InSAR technology with low accuracy of landslide monitoring, it is feasible to identify the landslides in ravine reservoir area.

4.2. Error Estimation

The D-InSAR technique uses phase measurements to obtain the characteristics of the target area and deformation information. An interferometric image contains topographic information, surface information, and phase delay caused by atmospheric activities that are sensitive to micro-deformation [23]. If the deformation is not caused by landslide movement, then it will directly influence the differential results.

Errors are produced in many aspects of SAR imaging and differential interferometry processing. Atmospheric effects, particularly on atmospheric water vapor, are among the main errors in InSAR [24]. Moderate-Resolution Imaging Spectroradiometer (MODIS) satellite data were used to retrieve atmospheric water vapor directly from remote sensing images and to remove atmospheric effects from the monitoring results to solve the aforementioned problem [25].

CR-InSAR and PS-InSAR are used to quantitatively analyze the error value. PS–InSAR technique will be used to eliminate errors when data accumulate to a certain amount [26]. PS points have high phase correlation and small pixels in a long time interval, although baseline length exceeds the critical baseline. CR points can overcome the limilations of place, including the lack of man-made objects and rocks. Monitoring deformations were considered as errors to analyze monitoring results of the PS points and CR points in stability region. Thus, the monitoring deformation from CR points and PS points is caused by errors, the displacement values are error values.

4.2.1. River as a Stable Point for Estimating Errors

As considered that the changes in PS were caused by rock and soil lifting or falling, whereas incident and reflection changes were caused by the atmospheric environment or orbital changes. Dispersion statistics represent the stability of the BS. Extremes characterized the changes in the BS. A geographic information system (GIS) software raster calculator was used to compute the BS extremes of eight images in 2010. A larger extreme indicates more unstable data, and vice versa.

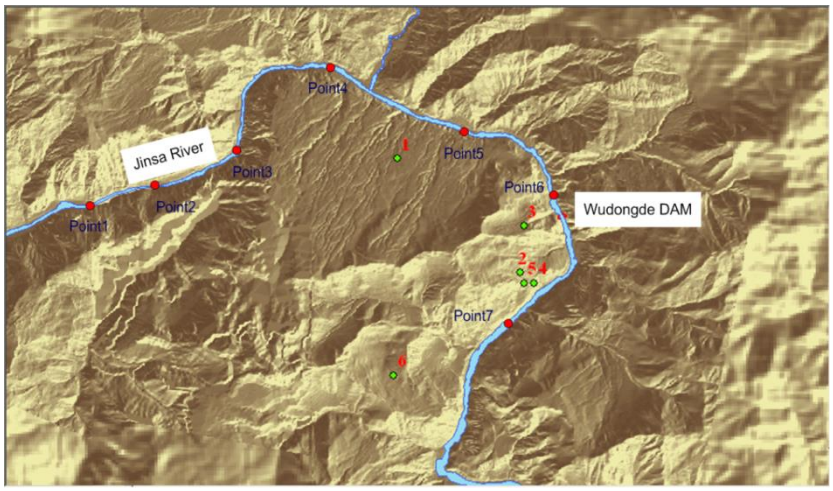

Figure 9. D-Insar Data Rivers Fixed Point Selected Area

This study considered the changes in the BS to be less than or equal to that of the river in the stability area. The main changes were caused by the atmospheric environment or orbital changes. Seven selected areas near the Jinsha River, each measuring 6m×6m, were observed to study river data characteristics and attempted to select the equidistant point to better represent the variation in river's BS. The selected area is shown in Figure 9. The changes in the BS as Maximum (Max), Minimum (Min), and Mean in the selected area as shown in Figure 10.

The chart indicates the following conditions.

1. The BS associated with specific morphological conditions of rivers is small.
2. The changes are small at different time periods considering that the BS of the river is stable.
3. Moving tendency of BSs are basically the same in the selected area, except that in image No. 5, which is caused by the atmospheric environment or orbital changes.

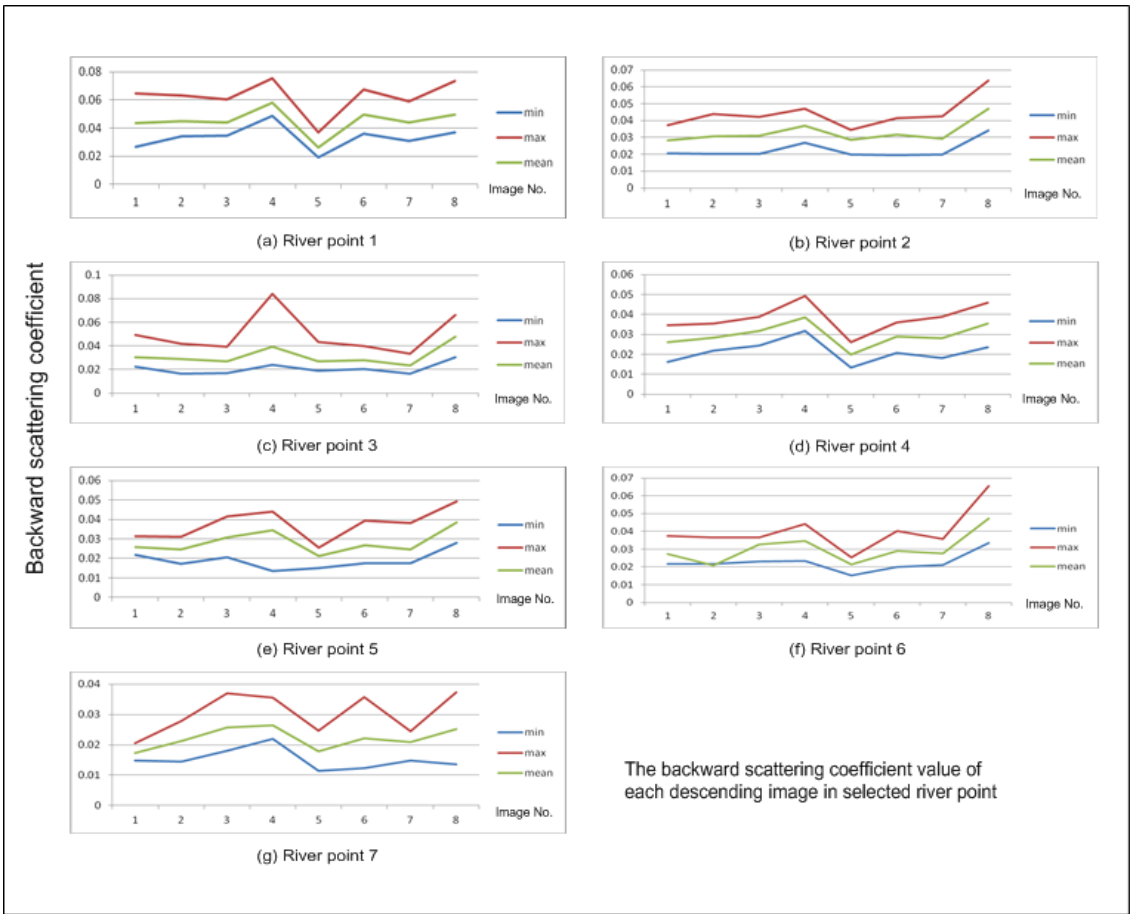

Figure 10. Rivers Fixed Point Backward Scattering Coefficient Change Chart

The total grids were 39875, Min was 0.035, Max was 4.620, and Mean was 0.204, as computed by the raster calculator. The BSs that were less than 0.25 were centralized in the river area, which indicates that the coefficients with such values were located in the stable area. The movement in the stable area was not caused by landslide movement. The error value was approximately 4cm to 6cm, which was caused by the atmospheric environment or orbital changes. The minimum value of landslide movement that can be identified by D-InSAR was 4 cm to 6cm. Given the terrain and topography features, the error value was larger than the theoretical error value.

4.2.2. CR Point Error Analysis

The CR points (1m×1m) were laid around the Jinpingzi landslide to study its peripheral data. The CR points were considered as the stable point that did not affect surface movement [27]. We analyzed vertical and horizontal displacements after SAR data processing. The results are shown in Figure 11, whereas the CR points are shown in Figure 9.

The CR points were the stable point, wherein surface movement did not occur. SAR movement was caused by the atmospheric environment or orbital changes. The error value was approximately 5cm, which is consistent with the error value based on the result of the river point analysis.

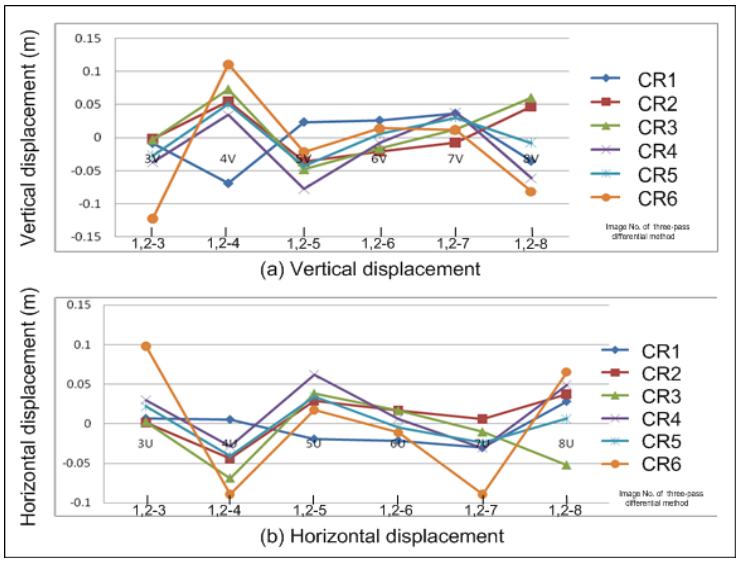

Figure 11. CR Point Displacement Changes Curve, (a) Vertical Displacement Changes Curve (b) Horizontal Displacement Changes Curve

5. Conclusion

Through the comprehensive analysis of D-InSAR data and topographic features in ravine reservoir area, there are several conclusions as follows: First, when the LIA larger than 50°, CC and BS are reduced significantly. The interference results are poor, regional area cannot be trusted. Using single shooting model in the same area cannot cover the whole area. Using the LIA of 50°, CC of 0.18 and overlapping orbit shooting modes, SAR data credible zone can covered the entire zone. Second. River as the stable points and CR points are used to error analysis, the systematic error caused by atmospheric conditions is about 4cm to 6cm. In the other wards, it is hard to detect the landslide movement by D-InSAR technique in this error range. This study proposed qualitatively error value based on D-InSAR data analysis and analyze the causes of error, to lay the foundation for the landslide early detection theory.

Acknowledgements

This project is supported by the Changjiang Institute of Survey, Planning, Design, and Research, as well as the National Natural Science Foundation of China (Grant No. 41372370).

References

[1] Zhang J, Xu JT, Kong LM, Feng G. The application of landslide deformation monitoring technology. *Beijing Surveying and Mapping*. 2009; 2: 47-50.
[2] Feng C, Zhang J, Li SH, Xu LK. A review of the latest development of landslide deformation monitoring techniques. *The Chinese Journal of Geological Hazard and Control.* 2011; 22(1): 11-16.
[3] Li CL, Zhang JQ, Guo BY. New method of landslide monitoring based on close-range photogrammetry. *Computer Engineering and Applications.* 2011; 47(3): 6-8.

[4] Zhang J, Hu GD, Luo NB. Landslide monitoring by InSAR. *Chinese Journal of Engineering Geophysics.* 2004; 1(2): 148-153.
[5] Gabriel AK, Goldstein RM, Zebker HA. Mapping small elevation changes over large areas: differential radar interferometry. *Journal of Geophysical Research.* 1989; 94(B7): 9183-9191.
[6] Achache J, Fruneau B, Delacourt C. *Applicability of SAR interferometry for operational monitoring of landslides.* Proceedings of the Second ERS Applications Workshop. London. 1995: 165-168.
[7] Berardino P, Costantini M, Franceschetti G, Iodice A, Petranera L, Rizzo V. Use of Differential SAR interferometry in monitoring and modelling large slope instability at Maratea (Basilicata, Italy). *Engineering Geology.* 2003; 68: 31-51.
[8] Colesanti F, Ferretti A, Prati C, Rocca F. Monitoring landslides and Tectonic Motions with the permanent scatterers technique. *Engineering Geology*. 2003; 68(1-2): 3-14.
[9] Singhroy V, Molch K. Characterizing and monitoring rockslides from SAR techniques. *Advances in Space Research*. 2004; 33: 290-295.
[10] Catani F, Farina P, Moretti S, Nico G, Strozzi T. On the application of SAR interferometry to geomorphological atudies: estimation of landform attributes and mass movements. *Geomorphology*. 2005; 66(1-4): 119-131.
[11] Singhroy V, Couture R, Molch K, Poncos V. *InSAR monitoring of post-landslide activity.* In Proc. International Geoscience and Remote Sensing Symposium (IGARSS). Denver, USA. 2006: 1635-1638.
[12] Li DR, Zhou YQ, Ma HC. Principles and applications of interferometry SAR. *Science of Surveying and Mapping*. 2000; 25(1): 9-12.
[13] Yao GQ, Mu JQ. D-InSAR technique for land subsidence monitoring. *Earth Sci Front.* 2008; 15(4): 239-243.
[14] Wu T, Wang C, Zhang H. A review on latest differential InSAR resesrches. *Remote Sensing Information*. 2007; 1: 84-89.
[15] Ge Y, Wang JF, Liang Y, Wang ZS. Study on the relationship of phase uncertainties, position uncertainties and gray uncertainties and the pixel uncertainty of SAR original image. *Journal of Remote Sensing*. 2003; 7(4): 285-291.
[16] Li XW, Guo HD, Li Z. DEM generation and accuracy analysis on rugged terrain using ENVISAT/ASAR multi-angle InSAR data. *Journal of Remote Sensing.* 2009; 02: 276-281.
[17] Zhang JX, Wei JJ, Zhao Z, Huang GM. Color orthophoto map generation based on Multi-direction and Multi-polarization SAR data fusion. *Acta Geodaetica et Cartographica Sinica.* 2011; 40(3): 276-282.
[18] Bao YS, et al. A semi-empirical model for correction of terrain influences in SAR backscattering. *Acta Geodaetica et Cartographica Sinica*. 2011; 40(4): 483-494.
[19] Huang JH, Xie MW, Wang ZF, Liu XY, Fu Q. Research on the DEM precision of canyon acquired by InSAR technique. *Remote Sensing Information*. 2012; 1: 62-67.
[20] Huang Y. Research on surface deformation detecting by D-InSAR. Dissertation. *PLA Information Engineering University.* 2009.
[21] Zheng MX, Fukuyama K, Sanga-Ngoie K. Application of InSAR and GIS techniques to ground subsidence assessment in the Nobi Plain, Central Japan. *Remote sensing.* 2014; 14(1): 492-509.
[22] Gerardo, et al. Analysis with C- and X-band satellite SAR data of the Portalet landslide area. *Landslide*. 2011; 8(2): 195-206.
[23] Jehle M, Perler D, Small D, Schubert A, Meier E. Estimation of atmospheric path delays in TerraSAR-X data using models vs. measurements. *Remote Sensing*. 2008; 8(12): 8479-8491.
[24] Xu Y, Yue DJ. Quantitative analysis of atmospheric delay error in InSAR and D-InSAR data. *Processing Site Investigation Science and Technology*. 2013; 4: 20-23.
[25] Yang CS, Zhang Q, Zhang JQ. Reliability analysis of the atmospheric delay phase separated by InSAR time series method. *Journal of Geodesy and Geodynamics*. 2005; 35(1): 92-96.
[26] Frattini P, Crosta GB, Allievi J. Damage to buildings in large slope rock instabilities monitored with the PSInSAR technique. *Remote Sensing*. 2013; 5(10): 4753-4773.
[27] Xing XM. Study on monitoring the time series ground deformation in mining area based on CRInSAR and PSInSAR intergration. *Acta Geodaetica et Cartographica Sinica*. 2014; 43(8): 878.